A semiclassical theory for spectral line broadening in molecules*

Earl W. Smith

Gaseous Electronics Section, National Bureau of Standards, Boulder, Colorado 80302

M. Giraud

Universite De Provence, 13397 Marseille Cedex 4, France

J. Cooper

Joint Institute for Laboratory Astrophysics and Department of Physics and Astrophysics, University of Colorado, Boulder, Colorado 80309

(Received 7 April 1976)

A semiclassical S-matrix theory is developed and applied to spectral line broadening in linear molecules perturbed by atoms. This theory uses curved classical trajectories determined by the isotropic part of the atom–molecule interaction and the S-matrix is treated to all orders in the interaction. Numerical calculations can be made rather easily even for high quantum numbers. The theory is least accurate for very low quantum numbers, but even then calculations agree to within 10% with close coupling results where comparisons could be made. Comparisons were also made with other theoretical approaches using model potentials and with experiment using *ab initio* potential surfaces.

I. INTRODUCTION

The width and shift of spectral lines are often used as a probe for measuring the pressure and temperature of gases as well as for various relaxation and energy transfer processes. In recent years, the most commonly used theory for neutral gases (where charged particle densities are negligible) is the impact theory developed by Anderson[1] and extended by Baranger.[2] In this theory, the radiation is perturbed by a random sequency of nonoverlapping binary collisions. The half-width at half-maximum (HWHM) of an isolated vibration–rotation line is then given by[3]

$$w_{v'j',vj} = 2\pi n \int_0^\infty u f(u)\, du \int_0^\infty b\, db \times \left[1 - \mathrm{Re} \sum_{m_a m_b m_a' m_b' q} (-1)^{m_a - m_b} \begin{pmatrix} j & j' & 1 \\ -m_b & m_b' & q \end{pmatrix} \begin{pmatrix} j & j' & 1 \\ -m_a & m_a' & q \end{pmatrix} \langle vjm_a | S(u,b) | vjm_b \rangle \langle v'j'm_a' | S(u,b) | v'j'm_b'^* \rangle \right], \quad (1.1)$$

where n is the density of perturbing particles, u is the relative velocity of radiator and perturber, $f(u)$ is a Maxwellian velocity distribution, and $S(u,b)$ is the classical path S-matrix for a binary collision with impact parameter b and velocity u. In this expression, the translational motion of all particles is treated classically; that is, the particles are assumed to follow classical trajectories determined by some interaction potential. The internal states of the particles (e.g., vibration, rotation, etc.) are treated quantum mechanically and in Eq. (1.1) are described by the quantum numbers (v, j, m). One could also include internal perturber states in Eq. (1.1), but in this paper we are only interested in perturbers which remain in their ground state (i.e., noble gas atoms); thus, for simplicity, we have not specified any perturber quantum numbers. The derivation of Eq. (1.1) and its conditions for validity have been discussed at length in the literature (e.g., see Ref. 3) and will not be discussed here.

In this paper we will discuss a new method of calculating the classical path S-matrix for rotation–vibration transitions and contrast our approach with the commonly used perturbation approach known as "Anderson theory," the "semiclassical" theory of Neilsen and Gordon,[4] the inelastic approximation of Murphy and Boggs,[5] as well as completely classical and completely quantum mechanical (i.e., close coupling) calculations. For a review of these and other theoretical approaches, see Rabitz.[3]

In the Anderson theory, the S-matrix is approximated by a second order expansion in the interaction potential and the classical trajectories are taken to be straight lines. This method requires some type of impact parameter cutoff, otherwise the colliding particles would pass through one another for small impact parameters, and the approximate S-matrix would diverge. This physically unrealistic situation is avoided by replacing the integral over small impact parameters by a hard sphere collision cross section, πb_0^2, or something similar. In the literature, one finds a countless variety of cutoff procedures, and by trying one after another, it is eventually possible to make a calculation agree with a given experiment (e.g., see Rabitz[3] or Bouanich and Haeusler[6]). Unfortunately, the calculations are very sensitive to the cutoff procedure and there is no single procedure which will describe a large number of different experiments. Thus, it is quite clear that with this method of calculation, the physically unrealistic impact

parameter cutoff is obscuring all the information about collision dynamics and interaction potentials which one hopes to obtain from line broadening.

Our method of calculating the classical path S-matrix employs curved trajectories. These trajectories are determined by the spherically symmetric part V_0 of the interaction potential. The S-matrix is then calculated to all orders in the interaction potential (thus preserving its unitarity). With such realistic classical trajectories there are no unphysical divergences resulting from two particles passing through one another. Further, when the interaction potential becomes very large, the second order expansion used in the Anderson theory breaks down, whereas our calculation to all orders in the interaction remains valid. Thus it is not necessary to introduce an impact parameter cutoff in our method. Our approach is quite similar to that used by Neilsen and Gordon[4] except that they used a numerical solution of the time dependent Schrödinger equation to obtain the S-matrix, whereas we use a numerical approximation involving the rotational quantum number j to obtain an analytic solution. Our approach is therefore much simpler and permits calculations for large values of j.

To illustrate our approach and the accuracy attainable using it and to permit a detailed comparison with other theoretical methods, we have performed calculations for several rotation lines in HCl, CO, and CO_2 perturbed by He and Ar.

II. THE CLASSICAL PATH S-MATRIX

Our method of calculation is based on an expression for the S-matrix which employs classical trajectories for the relative motion of the colliding particles. Such expressions have been derived by Cross[7] and by Smith *et al.*[8] In these derivations, the radiator–perturber interaction is written in the form

$$V = V_0 + V' \ , \tag{2.1}$$

where V_0 represents the spherically symmetric part of the interaction (which is diagonal in vibration–rotation states), and V' denotes the rest of the interaction. Translational scattering states $\phi_{\mathbf{p}}$ are obtained by solving the Schrödinger equation for V_0 only. Classical path results then follow when one evaluates matrix elements of V' by the method of stationary phase; for example,

$$\int d\mathbf{r}\, \phi_{\mathbf{p}}(\mathbf{r}, t)\, V'(\mathbf{r})\, \phi_{\mathbf{p}'}(\mathbf{r}, t) \simeq \delta_{\mathbf{p},\mathbf{p}'}\, V'(\mathbf{r}_{\mathbf{p}}(t)) \tag{2.2}$$

where $\mathbf{p}$ and $\mathbf{p}'$ denote the relative momenta when the particles are infinitely far apart and $\mathbf{r}_{\mathbf{p}}(t)$ denotes the classical trajectory for motion in V_0. Following the derivation given in Secs. 2 and 3 of Ref. 8, one obtains the following expression:

$$\langle \mathbf{p}\, vjm \,|\, S \,|\, \mathbf{p}'\, vj'm' \rangle = \langle \mathbf{p} \,|\, S_0 \,|\, \mathbf{p}' \rangle \langle vjm \,|\, S'(\mathbf{r}_{\mathbf{p}}) \,|\, vj'm' \rangle \ , \tag{2.3}$$

with the S' matrix elements given by the time ordered series

$$\langle vjm \,|\, S'(\mathbf{r}_{\mathbf{p}}) \,|\, vj'm' \rangle = \delta_{jj'}\, \delta_{mm'} - i \int_{-\infty}^{\infty} dt\, e^{i\omega_{jj'}t} \langle vjm \,|\, V'(\mathbf{r}_{\mathbf{p}}(t)) \,|\, vj'm' \rangle$$
$$- \sum_{j''m''} \int_{-\infty}^{\infty} dt\, e^{i\omega_{jj''}t} \langle vjm \,|\, V'(\mathbf{r}_{\mathbf{p}}(t)) \,|\, vj''m'' \rangle \int_{-\infty}^{t} dt'\, e^{i\omega_{j''j'}t'} \langle vj''m'' \,|\, V'(\mathbf{r}_{\mathbf{p}}(t')) \,|\, vj'm' \rangle + \cdots \ . \tag{2.4}$$

For convenience, all $\hbar$ factors have been absorbed in V [see Eqs. (2.7)–(2.11)]. The matrix S_0 is comparable to the term $\exp(2i\eta_0)$ obtained by Cross.[7] In quantum mechanical expressions for the half-width (e.g., Sec. 3B of Ref. 8), one always has the matrix product SS^*. Thus, when Eq. (2.3) is used for S, the factors $S_0 \simeq \exp(2i\eta_0)$, which describe purely translational effects, cancel out [since the same trajectory is used for both upper and lower states; see Eq. (3.15) of Ref. 8]. The matrix S' describes transitions between the rotational states induced by the collision; transitions between different vibrational levels have been ignored since they are much weaker than the rotational transitions [owing to the $\exp(i\omega_{v'v}t)$ factors which would appear in Eq. (2.4)]. The S'-matrix is comparable to the factor $\exp(2i\eta_0)$ obtained by Cross, except that our result is a time ordered exponential. Finally, to obtain the expression given in Eq. (1.1) it is necessary to perform an angular average over the relative directions of $\mathbf{p}$ and $\mathbf{p}'$. This angular average reduces the matrix product $S'(\mathbf{r}_{\mathbf{p}})\, S'(\mathbf{r}_{\mathbf{p}'})^*$ to $S(u, b)\, S^*(u, b)$ multiplied by two $3j$ symbols summed over azimuthal quantum numbers m [see Eq. (1.1)]. Note that this angular average (or sum over m states) leaves the final expression invariant to further rotations of the coordinate frame. The matrix elements of $S(u, b)$ are thus given by a time ordered series equivalent to that in Eq. (2.4). For simplicity, these matrix elements are written in the form

$$\langle vjm \,|\, S(u, b) \,|\, vj'm' \rangle = \langle vjm \,|\, \mathcal{O}\, e^{-i\eta'} \,|\, vj'm' \rangle \ , \tag{2.5}$$

$$\langle vjm \,|\, \eta' \,|\, vj'm' \rangle = \int_{-\infty}^{\infty} dt\, e^{i\omega_{jj'}t} \langle vjm \,|\, V'\{r(t), \Theta(t), \phi\} \,|\, vj'm' \rangle \ , \tag{2.6}$$

where $\mathcal{O}$ is the time ordering operator and the coordinates $\{r(t), \Theta(t), \phi\}$, which are functions of the impact parameter b and velocity u, describe the classical trajectory in the center of mass frame.

For the atom–linear molecule collisions considered in this paper, we take

$$V_0(r) = \frac{4\epsilon}{\hbar}\left[\left(\frac{d}{r}\right)^{12} - \left(\frac{d}{r}\right)^{6}\right] \ , \tag{2.7}$$

$$V'(r, \Theta) = \sum_l P_l(\cos\Theta)\, V_l(r) = \left(\frac{4\pi}{2l+1}\right) \sum_{lm} Y_m^{l*}(\Theta(t), \phi)\, Y_m^l(\Theta', \phi')\, V_l(r(t)) \ , \tag{2.8}$$

where Θ is the angle between the radiator–perturber internuclear axis and the molecular axis; (Θ', ϕ') denote the orientation of the molecule relative to a space fixed

frame; and $(\Theta(t), \phi)$ are the trajectory coordinates

$$V_1(r) = \frac{4\epsilon}{\hbar}[R_1(d/r)^{12} - A_1(d/r)^7] \ , \tag{2.9}$$

$$V_2(r) = \frac{4\epsilon}{\hbar}[R_2(d/r)^{12} - A_2(d/r)^6] \ , \tag{2.10}$$

$$V_l(r) = \frac{4\epsilon}{\hbar}[R_l(d/r)^{12} - A_l(d/r)^6] \quad l \geq 3 \ . \tag{2.11}$$

We have chosen a $(d/r)^{12}$ repulsive potential rather than an exponential form only for convenience. For thermal energy scattering, most exponential potentials can be adequately approximated by $(d/r)^{12}$ and the trajectory calculations are slightly simpler with the latter. The r^{-7} attraction in $V_1(r)$ is chosen to conform with conventional usage [for example, Eq. (4) of Neilsen and Gordon][4] which is based on the known functional dependence at large r. However, it should be noted that all $V_l(r)$ can be adequately represented by the 6–12 form since atom–molecule line broadening calculations are relatively insensitive to the exact $r \to \infty$ asymptote. In fact, the $r \to \infty$ asymptotes of potentials obtained from line broadening or molecular beam and transport data often differ with calculated polarizabilities by a factor of 2 or so (for example, Pack, Ref. 9).

Equation (2.8) is adequate only for pure rotation transitions. For vibration–rotation lines, the polarizabilities of the initial and final states may be somewhat different owing to the change in the vibrational quantum number. The repulsive part of the interaction may also be affected owing to the fact that vibrational excitation tends to increase the size of the molecule. In order to take these effects into account, one may wish to add an isotropic term to Eq. (2.8).

$$V_0^{(\mathrm{vib})} = \frac{4\epsilon'}{\hbar}\left[\left(\frac{d'}{r}\right)^{12} - \left(\frac{d'}{r}\right)^6\right] , \tag{2.12}$$

where ϵ' and d' are functions of the vibrational quantum number; A_1, A_2, R_1, R_2, etc., may have a slight dependence on vibration quantum number (see Giraud *et al.*, Ref. 10).

III. THE PEAKING APPROXIMATION

We next consider the phase integral η' which is given by Eqs. (2.6) and (2.8) as

$$\langle jm|\eta'|j'm'\rangle = \sum_{l\mu}\left(\frac{4\pi}{2l+1}\right)\langle jm|Y_\mu^l|j'm'\rangle \times \int_{-\infty}^{\infty} e^{i\omega_{jj'}t} Y_\mu^{l*}(\Theta(t), \phi)\, V_l(r(t))\, dt \ , \tag{3.1}$$

where for simplicity we have suppressed the vibrational quantum number.

The time $t = 0$ is chosen to be the time of closest approach [i.e., the time when $r(t)$ is smallest]. Both of the radial functions r^{-12} and r^{-6} are sharply peaked at $t = 0$, and the "resonance factor" $\exp(i\omega_{jj'}t)$ can only further enhance this peaking. We therefore make the "peaking approximation" by expanding the angular terms $Y_\mu^l(\Theta(t), \phi)$ about $t = 0$ and retaining only the "zeroth order" term. That is, we replace $Y_\mu^l(\Theta(t), \phi)$ by $Y_\mu^l(\Theta_0, \phi)$ where Θ_0 is the angle at the time of closest approach:

$$\langle jm|\eta'|j'm'\rangle \simeq \sum_{l\mu}\left(\frac{4\pi}{2l+1}\right)\langle jm|Y_\mu^l|j'm'\rangle\, Y_\mu^{l*}(\Theta_0, \phi) \times \int_{-\infty}^{\infty} e^{i\omega_{jj'}t} V_l(r(t))\, dt \ . \tag{3.2}$$

This peaking approximation has been discussed in detail by Roberts (Ref. 11).

Since Eq. (1.1) is rotationally invariant, we may rotate through the Euler angles $(-\phi, -\Theta_0, 0)$ for a given b and u. That is, we rotate to a coordinate frame where the phase shift matrix becomes

$$\langle jm|\eta'|j'm'\rangle = \delta_{mm'}\sum_l \sqrt{\frac{4\pi}{2l+1}}\langle jm|Y_0^l|j'm\rangle \times \int_{-\infty}^{\infty} e^{i\omega_{jj'}t} V_l(r(t))\, dt \ , \tag{3.3}$$

where we have used $Y_\mu^l(0, 0) = \delta_{\mu 0}\sqrt{(2l+1)/4\pi}$ and the fact that the Y_0^l operator is diagonal in m.[12,13]

IV. EVALUATION OF THE CLASSICAL PATH *S*-MATRIX

In order to evaluate the S-matrix elements, we first evaluate the matrix elements of Y_0^l required by Eq. (3.3).

From Edmonds[12] (pp. 59 and 122), we obtain an approximate expression for the $3j$ symbols so the matrix elements of Y_0^l may be given by

$$\langle jm|Y_0^l|j'm\rangle = (-1)^m\sqrt{\frac{(2j+1)(2l+1)(2j'+1)}{4\pi}} \times \begin{pmatrix} l & j' & j \\ 0 & 0 & 0 \end{pmatrix}\begin{pmatrix} l & j & j' \\ 0 & m & -m \end{pmatrix} \simeq \sqrt{\frac{2l+1}{4\pi}}\frac{(l-\Delta j)!}{(l+\Delta j)!}\, P_l^{\Delta j}(0)\, P_l^{\Delta j}(\cos\alpha) , \tag{4.1}$$

where $\Delta j = j - j'$ and P_l^m are associated Legendre polynomials. According to Edmonds, $\cos\alpha = m/\sqrt{j(j+1)}$, but we have used $\cos\alpha = m/(j+\frac{1}{2})$ since it is just as accurate and more convenient in our computer program. In the Appendix we show that the error introduced by the approximation in Eq. (4.1) is at most the order of $(\Delta j/j)^2$.

The frequency factor $\omega_{jj'}$ which appears in Eq. (2.4) may be approximated by

$$\begin{aligned}\omega_{jj'} &= 2\pi cB[j(j+1) - j'(j'+1)] \\ &= 2\pi cB(j + j' + 1)\,\Delta j \\ &= 2\pi cB(2j+1)\Delta j[1 + \Delta j/(2j+1)] \\ &\simeq \omega\Delta j \ ,\end{aligned} \tag{4.2}$$

where B is the rotational constant. It will be assumed that ω defined by $2\pi cB(2j+1)$ is essentially constant, that is, the Δj changes in j are small compared with j itself. This approximation was tested by using the next higher order approximation to $\omega_{jj'}$ [i.e., terms of order $(\Delta j/j)^2$] which had less than a 1% effect on our calculations (see also the discussion in the Appendix).

We next define a function $F_{j-j'}(t)$ by

$$F_{\Delta j}(t) = \frac{(l-\Delta j)!}{(l+\Delta j)!}\ (0)\ P_l^{\Delta j}\left(\frac{m}{j+\frac{1}{2}}\right) V_l(r(t)) \quad . \tag{4.3}$$

Notice that $F_{\Delta j}$ also depends on j through the argument of the Legendre polynomial; this will be discussed further following Eq. (4.13). Using Eq. (4.3), Eq. (3.1) becomes

$$\langle jm|\eta'|j'm\rangle = \delta_{mm'} \int_{-\infty}^{\infty} F_{\Delta j}(t) \exp(it\omega\Delta j)\, dt \quad . \tag{4.4}$$

The S-matrix in Eq. (2.5) may now be written in the form

$$\langle jm|S(u,b)|j'm'\rangle = \delta_{mm'} \sum_{n=0}^{\infty} (-i)^n \langle jm|I_n|j'm\rangle \,, \tag{4.5}$$

where $I_0 = 1$, and

$$\langle jm|I_1|j'm\rangle = \int_{-\infty}^{\infty} dt\, F_{j-j'}(t) \exp\{i\omega(j-j')t\} \,,$$

$$\langle jm|I_n|j'm\rangle = \sum_{j_2 j_3 \cdots j_n} \int_{-\infty}^{\infty} dt_1 F_{j-j_2}(t_1) \exp\{i\omega(j-j_2)t_1\}$$

$$* \int_{-\infty}^{t_1} dt_2 F_{j_2-j_3}(t_2) \exp\{i\omega(j-j_2)t_1\} \cdots \int_{-\infty}^{t_{n-1}} dt_n F_{j_n-j'}(t_n) \exp\{i\omega(j_n-j')t_n\} \quad . \tag{4.6}$$

We next multiply the right side of Eq. (4.6) by

$$1 = \sum_{j_1} \delta_{j,j_1} = \frac{1}{2\pi} \sum_{j_1} \int_{-\pi}^{\pi} e^{is(j-j_1)}\, ds \tag{4.7}$$

so that we can replace j by j_1 in Eq. (4.6). Then changing summation variables from $(j_1, \ldots, j_n)$ to $(\delta_1, \ldots, \delta_n)$, where

$$\begin{aligned} j_n &= j' + \delta_n \,, \\ j_{n-1} &= j' + \delta_n + \delta_{n-1} \,, \\ &\vdots \\ j_1 &= j' + \delta_n + \delta_{n-1} + \cdots + \delta_1 \,, \end{aligned} \tag{4.8}$$

Eq. (4.6) finally becomes

$$\langle jm|I_n|j'm\rangle = \frac{1}{2\pi} \sum_{\delta_1 \cdots \delta_n} \int_{-\pi}^{\pi} \exp\{is(j-j'-\delta_1-\cdots-\delta_n)\} ds$$

$$\times \int_{-\infty}^{\infty} F_{\delta_1}(t_1) \exp\{i\omega\delta_1 t_1\} dt_1 \int_{-\infty}^{t_1} F_{\delta_2}(t_2) \exp\{i\omega\delta_2 t_2\} dt_2 \cdots \int_{-\infty}^{t_{n-1}} F_{\delta_n}(t_n) \exp\{i\omega\delta_n t_n\} dt_n \quad . \tag{4.9}$$

Note that while $j_1, \ldots, j_n$ were summed over the range 0 to ∞, the variables $\delta_1, \ldots, \delta_n$ are summed over the range $-\infty$ to $+\infty$.

Using the identity

$$\sum_{\delta_1\delta_2} \int_{-\infty}^{\infty} dt_1 f_{\delta_1}(t_1) \int_{-\infty}^{t_1} dt_2 f_{\delta_2}(t_2) = \frac{1}{2} \sum_{\delta_1\delta_2} \left[\int_{-\infty}^{\infty} dt_1 f_{\delta_1}(t_1) \int_{-\infty}^{t_1} dt_2 f_{\delta_2}(t_2) + \int_{-\infty}^{\infty} dt_2 f_{\delta_2}(t_2) \int_{t_2}^{\infty} dt_1 f_{\delta_1}(t_1) \right]$$

$$= \frac{1}{2} \sum_{\delta_1\delta_2} \int_{-\infty}^{\infty} dt_1 f_{\delta_1}(t_1) \int_{-\infty}^{\infty} dt_2 f_{\delta_2}(t_2) \tag{4.10}$$

or, in general,

$$\sum_{\delta_1\delta_2\cdots\delta_n} \int_{-\infty}^{\infty} dt_1 f_{\delta_1}(t_1) \int_{-\infty}^{t_1} dt_2 f_{\delta_2}(t_2) \cdots \int_{-\infty}^{t_{n-1}} dt_n f_{\delta_n}(t_n) = \frac{1}{n!} \sum_{\delta_1\delta_2\cdots\delta_n} \int_{-\infty}^{\infty} dt_1 f_{\delta_1}(t_1) \int_{-\infty}^{\infty} dt_2 f_{\delta_2}(t_2) \cdots \int_{-\infty}^{\infty} dt_n f_{\delta_n}(t_n) \,. \tag{4.11}$$

Equation (4.9) becomes

$$\langle jm|I_n|j'm\rangle = \frac{1}{2\pi} \int_{-\pi}^{\pi} ds\, e^{is(j-j')} \frac{1}{n!} \left[\sum_{\delta} e^{-is\delta} \int_{-\infty}^{\infty} dt\, e^{i\omega t\delta} F_{\delta}(t) \right]^n \tag{4.12}$$

and Eq. (4.5) gives

$$\langle jm|S(u,b)|j'm'\rangle = (\delta_{mm'}/2\pi) \int_{-\pi}^{\pi} ds\, e^{is(j-j')} \exp\left[-l \sum_{\delta} e^{-is\delta} \int_{-\infty}^{\infty} dt\, e^{i\omega t\delta} F_{\delta}(t) \right] \,. \tag{4.13}$$

In deriving this result, we have again assumed that the increments $\delta_k = (j_k - j_{k-1})$ in the j quantum numbers are small compared with the j_k themselves. This was done when we replaced the sum over $(j_1, \ldots, j_n)$ by $(\delta_1, \ldots, \delta_n)$ and assumed that F_{δ_k} depends only on δ_k. In reality, F depends on j_k as well as $(j_k - j_{k-1})$ [see Eq. (4.3)]; by ignoring the former we are assuming that the incremental changes in j are small compared with j it-

self. This is rigorously correct for the $\Delta j = 0$ terms, and in the Appendix it is shown that the $\Delta j \neq 0$ terms introduce an error the order of $(\Delta j/j)^2$ or smaller. Equation (4.13) has also been obtained by Percival and Richards[14] by assuming that the quantum number is much larger than its incremental change. While this condition is also regarded as the "classical limit," we recall that we have not treated the azimuthal quantum number m in this manner because we were able to diagonalize the phase shift matrix η' in m. This is desirable since $|m|$ ranges from 0 to j and thereby includes some distinctly nonclassical values.

To proceed further, we note that $r(t)$ and $F_\delta(t)$ are even functions of t. This property reduces the t integral in Eq. (4.13) to a cosine transform. We therefore define a set of functions $K_\delta(\omega)$ by

$$K_0 = 2 \sum_l P_l^0(0)\, P_l^0\left(\frac{m}{j+\frac{1}{2}}\right) \int_0^\infty V_l(r(t))\, dt \quad , \tag{4.14}$$

and for $\delta > 0$

$$K_\delta(\omega) = 4 \sum_{l \geq \delta} \frac{(l-\delta)!}{(l+\delta)!}\, P_l^\delta(0)\, P_l^0\left(\frac{m}{j+\frac{1}{2}}\right) \times \int_0^\infty V_l(r(t)) \cos(\omega \delta t)\, dt \quad . \tag{4.15}$$

Our expression for the S-matrix, Eq. (4.13), finally becomes

$$\langle jm|S(u,b)|j'm\rangle = (\delta_{mm'}/2\pi) \int_{-\pi}^{\pi} ds\, e^{is(j-j')} \times \exp\left[-i \sum_{\delta \geq 0} \cos(\omega s \delta)\, K_\delta(\omega)\right] \quad . \tag{4.16}$$

As mentioned in Sec. II, one may wish to add an isotropic term $V_0^{(\mathrm{vib})}$ to the interaction in order to account for the effect of vibrational excitation [see Eq. (2.12)]. This correction simply adds the factor

$$K_0^{(\mathrm{vib})} = \int_0^\infty V_0^{(\mathrm{vib})}(r(t))\, dt \tag{4.17}$$

to the K_0 term already defined in Eq. (4.14).

V. THE LINEWIDTH

The expression for the linewidth, Eq. (1.1), is simplified by the fact that the S-matrix is diagonal in m:

$$w_{v'j',vj} = 2\pi n \int_0^\infty uf(u)\, du \int_0^\infty bdb\, \sigma_{vj,v'j'}(u,b)$$
$$= 2\pi n \int_0^\infty uf(u)\, du \int_0^\infty bdb \left[1 - \mathrm{Re} \sum_{mm'q} \begin{pmatrix} j & j' & 1 \\ -m & m' & q \end{pmatrix}^2 \langle vjm|S(u,b)|vjm\rangle \langle v'j'm'|S(u,b)|v'j'm'\rangle^*\right] \quad . \tag{5.1}$$

This equation also defines the unaveraged optical cross section $\sigma(u,b)$ which will be useful in comparing theoretical results.

Another interesting expression for the linewidth can be obtained by using the identities

$$\mathrm{Re}\langle vjm|S|vjm\rangle \langle v'j'm'|S|v'j'm'\rangle^* = \tfrac{1}{2}\{|\langle vjm|S|vjm\rangle|^2 + |\langle v'j'm'|S|v'j'm'\rangle|^2 - |\langle vjm|S|vjm\rangle - \langle v'j'm'|S|v'j'm'\rangle|^2\} \tag{5.2}$$

and

$$\sum_m |\langle vjm|S|vjm\rangle|^2/(2j+1) = 1 - \sum_m \{1 - |\langle vjm|S|vjm\rangle|^2\}/(2j+1) = 1 - \sum_m \sum_{v'j'm' \neq vjm} |\langle vjm|S|v'j'm'\rangle|^2/(2j+1) \quad . \tag{5.3}$$

Substituting these identities into Eq. (5.1), we obtain

$$w_{v'j',vj} = \tfrac{1}{2}(\nu_{vj}^{in} + \nu_{v'j'}^{in}) + \pi n \int_0^\infty uf(u)\, du \int_0^\infty bdb \sum_{mm'q} \begin{pmatrix} j & j' & 1 \\ -m & m' & q \end{pmatrix}^2 |\langle vjm|S|vjm\rangle - \langle v'j'm'|S|v'j'm'\rangle|^2 \quad , \tag{5.4}$$

where ν_{vj}^{in} is the total inelastic rate out of the level vj:

$$\nu_{vj}^{in} = 2\pi n \int_0^\infty uf(u)\, du \int_0^\infty bdb \sum_m [1 - |\langle vjm|S|vjm\rangle|^2]/(2j+1) \quad . \tag{5.5}$$

Equation (5.4) is interesting because it expresses the linewidth in terms of a purely inelastic contribution plus a coherence term which involves the difference of scattering amplitudes. The latter term, which is often neglected (for example, Murphy and Boggs),[5] contains the effect of elastic collisions which interrupt the phase of the radiator without quenching it. The elastic contribution can be quite important, especially in cases such as HCl–Xe where the vibrational broadening resulting from $K_0^{(\mathrm{vib})}$ is strong (e.g., Ref. 10). One must therefore exercise considerable care when using measured half-widths to infer inelastic cross sections.

VI. LINEWIDTH CALCULATIONS

A. General

Most of the calculations presented in this paper are based on model potentials which include anisotropy terms [see Eq. (2.8)] up to order $P_2(\cos\Theta)$. In such cases, we need only consider

$$K_0 = \tfrac{1}{2}\left[1 - 3\left(\frac{m}{(j+\frac{1}{2})}\right)^2\right] \int_0^\infty V_2(r(t))\, dt \quad , \tag{6.1}$$

$$K_1(\omega) = 2\sqrt{1-\left(\frac{m}{j+\frac{1}{2}}\right)^2}\int_0^\infty V_1(r(t))\cos(\omega t)\,dt \quad , \tag{6.2}$$

$$K_2(\omega) = \tfrac{3}{2}\left[1-\left(\frac{m}{j+\frac{1}{2}}\right)^2\right]\int_0^\infty V_2(r(t))\cos(2\omega t)\,dt \quad . \tag{6.3}$$

The S-matrix may then be evaluated by using the identity (Ref. 15, p. 361)

$$\exp(-iK\cos s) = J_0(K) + 2\sum_{l=1}^{\infty}(-i)^l J_l(K)\cos(ls) \tag{6.4}$$

[where $J_l(K)$ are Bessel functions of integer order i] and

$$\frac{1}{\pi}\int_{-\pi}^{\pi}\cos(ls)\cos(l's)\,ds = \delta_{l,l'} + \delta_{l,-l'} \quad . \tag{6.5}$$

The diagonal matrix elements of Eq. (4.16) are thus given by

$$\begin{aligned}\langle jm|S(u,b)|jm\rangle &= \frac{1}{2\pi}\int_{-\pi}^{\pi} ds\exp[-iK_0 - iK_1\cos(\omega s) - iK_2\cos(2\omega s)] \\ &= e^{-iK_0}\left[J_0(K_1)J_0(K_2) + 2\sum_{l=1}^{\infty}(-i)^{3l}J_{2l}(K_1)J_l(K_2)\right] \quad .\end{aligned} \tag{6.6}$$

The sum over Bessel functions in Eq. (6.6) converges very rapidly and it is usually necessary to include only three or four terms.

The recent theoretical potential surfaces which are based on the Gordon–Kim electron gas model[16] include important contributions from anisotropy terms as high as $P_5(\cos\Theta)$ and $P_6(\cos\Theta)$ (see Green,[17] Green, and Thaddeus,[18] Parker *et al.*).[19] For these potentials it is necessary to consider $K_5(\omega)$ terms as high as K_6. With such high order terms the expression for the S-matrix would be somewhat more complicated than Eq. (6.6). On the other hand, the higher order $K_5(\omega)$ terms represent a type of multiquantum transition whose effect decreases very rapidly with increasing order. For example, K_6 is proportional to a $\cos(6\omega t)$ transform of $V(r(t))$ which should be much smaller than the lower order terms such as K_0, K_1, etc. The primary effect of higher order anisotropies in V is thus found in their influence on the lower order terms such as K_0 and K_2. To verify this assertion we have performed calculations on CO_2–Ar and CO_2–He using the potentials of Ref. 19. For these potentials, V_0, V_2, and V_4 are roughly the same order of magnitude while higher terms V_6, V_8 and V_{10} are each an order of magnitude smaller than their preceeding terms. We have therefore used

$$K_0 = \tfrac{1}{2}\int_0^\infty dt\left[(1-3\mu^2)V_2 + \tfrac{3}{16}(35\mu^4-30\mu^2+3)V_4 - \tfrac{5}{64}(231\mu^6-315\mu^4+105\mu^2-5)V_6 + \tfrac{35}{2048}(6435\mu^8-12\,012\mu^6+6930\mu^4-1260\mu^2+35)V_8\right] , \tag{6.7}$$

$$K_2 = \tfrac{3}{2}(1-\mu^2)\int_0^\infty dt\left[V_2 + \tfrac{5}{12}(1-7\mu^2)V_4 + \tfrac{35}{64}(33\mu^4-18\mu^2+1)V_6 - \tfrac{105}{512}(143\mu^6-143\mu^4+33\mu^2-1)V_8\right]\cos(2\omega t) \quad , \tag{6.8}$$

$$K_4 = \tfrac{105}{96}(1-\mu^2)^2\int_0^\infty dt\left[V_4 + \tfrac{9}{20}(11\mu^2-1)V_6 + \tfrac{693}{2240}(65\mu^4-26\mu^2-1)V_8\right]\cos(4\omega t) \quad , \tag{6.9}$$

where $\mu = m/(j+\frac{1}{2})$. Since K_4 made about 0.5% change in the calculated half-widths, we did not bother to include a K_6 term. This result confirms our assertion that the higher order K_5 terms are relatively unimportant and the main effect of higher order anisotropies comes in via the K_0, K_1, and K_2 terms.

B. HCl-Ar

The pressure broadening of HCl by argon is an extremely valuable test case for a theory because (1) Neilsen and Gordon[4] have performed a numerical solution of Schrödinger's equation (using classical trajectories for the translational motion), which should be very accurate and thus may be used to test other classical path approaches, (2) there are now some very good theoretical potential surfaces for this system, and (3) there are experimental data ranging from low j (the 1–0 transition) where quantum effects are important to high j (the 11–10 transition) which is well into the classical region.

Neilsen and Gordon[4] have calculated the broadening, by argon, of the HCl pure rotation lines from the 1–0 transition of the 6–5 transition. They used classical paths determined by the isotropic part of the potential and solved the Schrödinger equation by a numerical technique. While this calculation is not as accurate as a fully quantum mechanical close coupling approach, it is certainly more accurate than our theory for low values of j. For high values of j, our results should agree with Neilsen and Gordon's,[4] as they do. This comparison thus gives an idea of the accuracy of our theory for low j, as well as providing a test of our numerical calculations.

In our calculation, we used the potential labeled $NC = 52$ by Neilsen and Gordon.[4] Our anisotropy parameters [see Eq. (2.9) and (2.10)] are $R_1 = 0.37$, $R_2 = 0.65$, $A_1 = 0.33$, $A_2 = 0.14$, which differ slightly from those given by Neilsen–Gordon[4] (on p. 4153) because they used an exponential repulsion rather than $1/r^{12}$. Our parameters were obtained by numerically fitting their potential.

Figure 1 compares the unaveraged cross section $\sigma(u,b)$ defined by Eq. (5.1) with that obtained by Neilsen-Gordon[4] for the 5–4 line at 400 K. In Table I, we have also listed various cross sections averaged over b and u which are defined by (again suppressing the vibrational quantum number)

$$\sigma_{jj'}(u) = 2\pi\int_0^\infty b\sigma_{jj'}(u,b)\,db \quad , \tag{6.10}$$

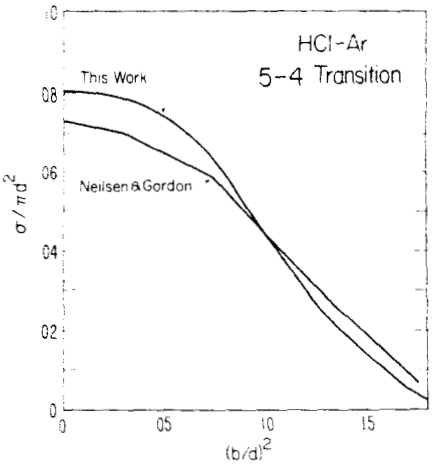

FIG. 1. Unaveraged HCl–Ar optical cross section [see Eq. (5.1)] for the 5–4 pure rotation line. The impact parameter is plotted in units of the hard sphere radius d [see Eq. (2.7)].

$$\sigma_{jj'} = \int_0^\infty u\sigma_{jj'}(u) f(u)\, du \left(\int_0^\infty uf(u)\, du \right)^{-1} , \qquad (6.11)$$

$$w_{jj'} = n\bar{u}\sigma_{jj'} , \qquad (6.12)$$

$$\bar{u} = \int_0^\infty uf(u)\, du . \qquad (6.13)$$

The excellent agreement between these results provides a useful confirmation of our theoretical approach and numerical calculations.

In Fig. 2, we have compared our calculations (averaged over velocity) with the experimental data of Pourcin,[20] Scott,[21] and Gebbie and Stone.[22] The agreement between theory and experiment is not important in itself since the anisotropy parameters were chosen by Neilsen and Gordon to give a reasonable fit to experimental data. The important point is that in calculations using Anderson theory, Giraud *et al.* (Ref. 10) were unable to fit the experimental data without unrealistic assumptions on the impact parameter cutoff (i.e., the cutoff was smaller than the hard sphere collision diameter), and they stressed the point that close collisions should be studied more carefully. From Fig. 1 it is clear that if one approximates $S(u, b)$ by unity for b less than some b_0, this value of b_0 will indeed be much smaller than the hard sphere diameter and will provide a very unrealistic approximation to the S-matrix.

In order to test the assumption of Murphy and Boggs[5]

TABLE I. HCl–Ar cross sections for pure rotation transitions (i.e., $v = v' = 0$) in Å^2. The unaveraged cross sections $\sigma_{j,j-1}(u)$ [Eq. (6.10)] are evaluated for two kinetic energies $E = mu^2/2k$ (where k is Boltzmann's constant). The averaged cross sections [Eq. (6.11)] are evaluated for a temperature of $T = 300$ K.

	Neilsen–Gordon			This work		
j	$E = 398$ K	$E = 776$ K	$T = 300$ K	$E = 404$ K	$E = 808$ K	$T = 300$ K
2	57.41	50.26	59.16	63.7	57.2	69.7
3	45.16	40.00	47.40	48.3	43.1	51.3
4	37.28	33.73	38.44	38.0	36.5	40.2
5	30.63	29.31	31.48	31.0	31.2	32.3
6	23.75	25.55	25.42	25.6	26.9	26.3

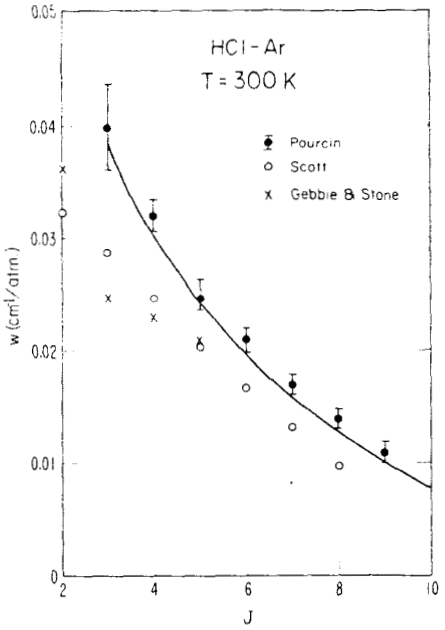

FIG. 2. Linewidths (HWHM) for $j \to j-1$ pure rotation transitions in HCl–Ar (atm – 101 325 Pa). Our theoretical results (solid line) are compared with the experimental data of Pourcin,[20] Scott[21], and Gebbie and Stone.[22]

that elastic broadening effects are negligible, we have evaluated the elastic and inelastic contributions to $\sigma_{j,j'}(u)$ [Eq. (6.10)] separately:

$$\sigma_{j,j'}(u) = \sigma^{\text{in}}_{j,j'}(u) + \sigma^{\text{el}}_{j,j'}(u) . \qquad (6.14)$$

The inelastic part is defined by [see Eq. (5.5)]

$$\sigma^{\text{in}}_{j,j'}(u) = \pi \int_0^\infty bdb \sum_m [2 - |\langle jm|S|jm\rangle|^2 - |\langle j'm|S|j'm\rangle|^2]/(2j+1) , \qquad (6.15)$$

so that the inelastic contribution to the half-width [see Eq. (5.4)] is

$$\tfrac{1}{2}(\nu^{\text{in}}_j + \nu^{\text{in}}_{j'}) = n \int_0^\infty \sigma^{\text{in}}_{j,j'}(u)\, uf(u)\, du . \qquad (6.16)$$

These cross sections are listed in Table II for HCl–Ar. From these data we conclude that, for HCl with its large rotational constant $B_e = 10.4$ cm^{-1}, it is not a good approximation to ignore elastic effects, especially for high j and low energies.

C. CO–He and HCl–He

Calculations were performed on CO–He and HCl–He using the potential proposed by Gordon.[23] The purpose of these calculations was to compare our results with those of the classical theories which are generally thought to be quite good for large j. Various calculations in which the internal states of the radiating molecule are treated classically have been made by Gordon,[23] Gordon and McGinnis,[24] and Fitz and Marcus.[25] Since our results disagree strongly with these classical and semiclassical calculations, it is fortunate that Green and Thaddeus[18] and Green and Monchick[26] have performed close coupling calculations for these systems using exactly the same potentials. The close coupling

TABLE II. Unaveraged HCl–Ar $j \rightarrow j-1$ cross sections [see Eq. (6.14)] for a kinetic energy $E = mu^2/2k = 404$ K.

j	$\sigma^{\text{in}}_{j,j-1}(u)$	$\sigma^{\text{el}}_{j,j-1}(u)$	$\sigma_{j,j-1}(u)$
2	51.3	12.4	63.7
4	30.5	7.5	38.0
6	19.9	5.7	25.6
8	10.3	4.5	14.8
10	4.1	3.4	7.5

technique, which is simply a numerical solution of the fully quantum mechanical Schrödinger equation (e.g., Ref. 27), is the most accurate technique available and provides the most reliable theoretical test.

As seen from Table III and Fig. 3, our results for CO–He agree very well (within 10%) with the close coupling results, but differ by as much as 50% from the classical results. The HCl–He results given in Table IV and Fig. 4 show a similar trend. In comparing the results for HCl–He, it should be noted that the results of Gordon, Fitz, and Marcus and our results have been averaged over velocity at a temperature of 300 K, whereas the close-coupling results of Green and Monchick were performed for a single velocity corresponding to a kinetic energy of 450 K. The comparison is nonetheless valid since the velocity averaged cross section at 300 K is essentially the same as the unaveraged cross section at 450 K due to the increase of $\sigma_{j,j'}(u)$ as a function of u (for example, note the corresponding data in Table III of Green and Monchick).[26] Again, our results differ by about 10% from the close coupling calculations and lie a factor of 2 or 3 below the classical theories. The classical results are clearly in error since they lie well above the close coupling calculation and the half-width decreases with increasing j (due to a decreased inelastic contribution).

This situation is rather surprising, since it is generally thought that the classical theory should be good for large j; furthermore, the classical HCl–Ar calculations

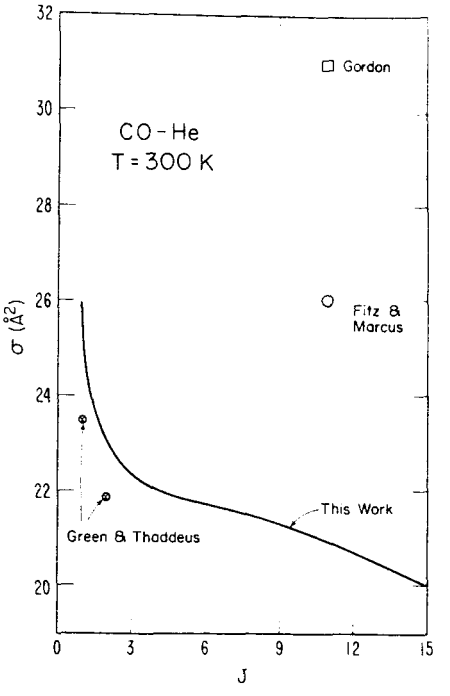

FIG. 3. Velocity averaged cross sections [Eq. (6.11)] for $j \rightarrow j-1$ transitions in Co–He at a temperature of 300 K. Our calculations are compared with those of Green and Thaddeus,[18] Gordon,[23] and Fitz and Marcus.[25] The data of Gordon and McGinnis[24] were not plotted since they are well off scale (see Table III).

of Fitz and Marcus agree quite well with our semiclassical results and those of Neilsen and Gordon. The explanation is perhaps found in the fact that both CO–He and HCl–He are completely dominated by inelastic broadening (see Tables III and IV) owing to their weak long range interaction (small well depth) and small reduced mass (resulting in higher velocities at a given temperature). The simple classical expression for the inelastic transition probability seems to be a weak point in the classical theory of Gordon[23] and even in the more recent theory of Fitz and Marcus[25]; it is necessary to replace the "primitive semiclassical" approximation by an "unformlike" approximation when the former breaks down (see Fitz and Marcus,[25] p. 3790).

TABLE III. CO–He $j \rightarrow j-1$ cross sections in Å^2. Unaveraged cross sections [Eqs. (6.10) and (6.14)] are evaluated for kinetic energy $E = mu^2/2k = 272$ K (k is Boltzmann's constant). The velocity averaged cross sections [Eq. (6.11)] are evaluated for a temperature of $T = 300$ K, and comparison is made with (a) Green and Thaddeus,[18] (b) Fitz and Marcus,[25] (c) Gordon,[23] and (d) Gordon and McGinnis,[24]

	Unaveraged, $E = 272$ K This work			Averaged, $T = 300$ K	
j	Inelastic	Elastic	Total	This work	Others
1	25.3	0.72	26.0	26.0	23.5(a) 36(d)
2	22.6	0.43	23.0	23.1	21.9(a) 34.6(d)
3	21.8	0.27	22.1	22.3	35.3(d)
4	21.7	0.18	21.9	22.0	36.8(d)
5	21.7	0.12	21.8	21.9	37.1(d)
6	21.6	0.09	21.7	21.7	36.7(d)
7	21.4	0.07	21.5	21.6	36.7(d)
8	21.3	0.05	21.4	21.5	36.0(d)
9	21.2	0.04	21.2	21.3	35.8(d)
10	21.0	0.04	21.0	21.	35.8(d)
11	20.8	0.03	20.8	20.9	26 (b), 31 (c), 36.0 (d)
12	20.6	0.03	20.6	20.7	35.6(d)

TABLE IV. HCl–He $j \rightarrow j-1$ cross sections in Å^2. Unaveraged cross sections [Eqs. (6.10) and (6.14)] are evaluated for kinetic energies $E = mu^2/2k$ (k is Boltzmann's constant) of 480 K and 450 K. Averaged cross sections, Eq. (6.11), are evaluated for a temperature of $T = 300$ K. Data are obtained from this work and (a) Green and Monchick,[26] (b) Fitz and Marcus,[25] and (c) Gordon.[23]

	This work, unaveraged $E = 480$ K			Unaveraged $E = 450$ K	Averaged $T = 300$ K	
j	Inelastic	Elastic	Total	Total	This work	Others
1	6.72	0.136	6.86	8.2(a)	7.46	14 (b), 17(c)
2	5.62	0.057	5.68	8.0(a)	6.28	13(b)
3	6.01	0.034	6.04	8.0(a)	6.49	
4	6.25	0.020	6.27	7.9(a)	6.53	
5	6.04	0.014	6.05		6.31	12(b), 14(c)
6	5.57	0.011	5.58		5.91	11.5(b)
7	5.00	0.008	5.01		5.43	
8	4.43	0.007	4.44		4.93	
9	3.88	0.005	3.89		4.43	
10	3.40	0.004	3.40		3.95	8(b), 10(c)

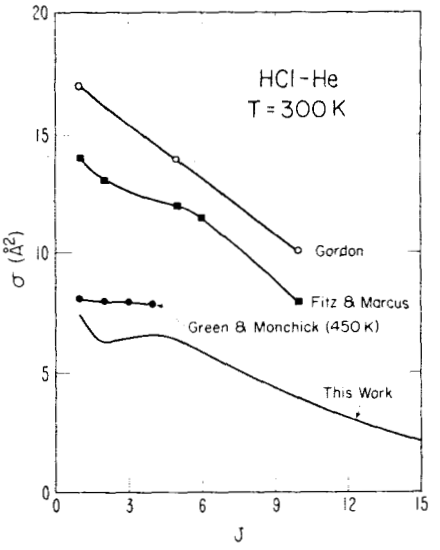

FIG. 4. Cross sections for $j \rightarrow j-1$ transitions in HCl–He. All calculations except those of Green and Monchick[26] are velocity averaged [Eq. (6.11)] at a temperature of 300 K. The unaveraged results of Green and Monchick at a kinetic energy $mu^2/2k = 450$ K (k is Boltzmann's constant) are expected to be roughly the same as the velocity averaged results (see discussion in Sec. VI. C).

D. CO_2–Ar and CO_2–He

The HCl–Ar, CO–He, and HCl–He calculations were used to provide a test of our theory by comparing it with other theoretical methods. The potentials used in those calculations were model potentials which were, in most cases, designed to provide agreement with experimental data. Comparisons with experiment would thus be somewhat misleading, especially since recent theoretical work has shown that higher order anisotropies must be included in the interaction potentials.

The purpose of the CO_2–Ar and CO_2–He calculations is to use some of the new theoretical potential surfaces based on the Gordon–Kim electron–gas model[16] and thus obtain a more realistic comparison with experimental data over a wide range of j values. We also wanted to see if the higher order K_5 terms would be negligible (as discussed in Sec. VI. A) and CO_2 provides a very stringent test of this approximation owing to its small rotational constant.

In our calculations we used the potentials obtained by Parker *et al.* (Ref. 19) fitting their $V_1(r)$ functions to 6–12 functions of the form shown in Eq. (2.11). For CO_2–Ar, our parameters were $\epsilon = 97.95$ K, $d = 3.86$ Å, $R_2 = 2.24$, $A_2 = 0.549$, $R_4 = 1.09$, $A_4 = 0.167$, $R_6 = 0.27$, $A_6 = 0.034$, $R_8 = 0.059$, $A_8 = 0.011$. Figure 5 shows the comparison of our calculations with the experimental results of Boulet *et al.* (Ref. 28) for j values ranging from 3 to 40. The dashed and dotted curves represent the effect of V_2 only and $V_2 + V_4$ terms. The solid curve represents the combined effect of V_2, V_4, V_6, and V_8. The addition of V_8 raised the curve less than 2% so the V_2, V_4, V_6 curve was not plotted. Ignoring the K_4 term [i.e., the $\cos(4\omega t)$ transform in Eqs. (4.16) and (6.9)] had less than 1% effect. Thus, the effect of higher order anisotropies in the potential is important up to the V_6 term, but the effect of these anisotropies enters only through the K_0 and K_2 terms in Eqs. (4.6), (6.7), and (6.8).

The agreement between theory and experiment is quite good, considering that there are no adjustable parameters in either the line shape theory or the *ab initio* potential. Nonetheless, it is clear that the theoretical results lie about 12% too low. This is probably due to vibrational effects which will enter via the $K_0^{(vib)}$ term discussed in Sec. II. Since these radiative transitions in CO_2 take place between two different vibrational modes, one would expect the vibrational effects to be relatively important, and they should be evaluated before drawing any final conclusions regarding the theoretical–experimental comparison.

As a further check on the vibrational broadening effect, we performed CO_2–He calculations. The contribution of vibrational broadening is much smaller for He perturbers than for Ar perturbers (see Refs. 10 and 29) because the smaller He polarizability makes long range forces less important; consequently, the CO_2–He broadening is dominated by short range forces which seem to be less affected by molecular vibration (for example, Tipping and Herman,[29] p. 893, *et seq.*). It was more difficult to fit the CO_2–He potentials of Parker *et al.*[19] to the 6–12 functions which we used in our computer program, and this difficulty introduced a ±2% uncertainty into our calculations. The parameters used were ($\epsilon = 20.25$ K, $d = 3.72$ Å, $R_2 = 2.85$, $A_2 = 0.71$, $R_4 = 1.44$, $A_4 = 0.07$, $R_6 = 0.52$, $A_6 = 0.10$, $R_8 = 0.13$, and $A_8 = 0.048$.

Our results, given in Fig. 6, agree quite well with the experimental data of Meyer *et al.*,[30] Judd,[31] and Abrams[32] for the 10 μm band and lie about 15% below the $P(20)$ measurement of Meyer *et al.*[30] for the 9 μm

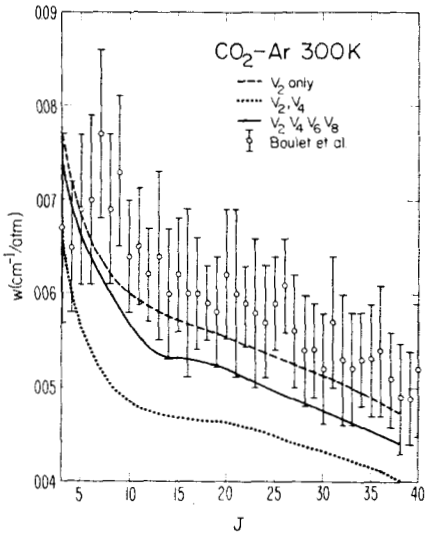

FIG. 5. Linewidths (HWHM) for $j \rightarrow j-1$ transitions in CO_2–Ar showing the contributions of higher order anisotropy terms in the potential. Terms higher than v_8 have a negligible effect on the linewidth (see discussion in Secs. VI. A and VI. D). Theoretical calculations (solid curve) compare favorably with the experimental results of Boulet *et al.*[28] The measurement of Meyer *et al.*, $w = 0.063$, for the $P(20)$ line was not plotted although it agrees with the data of Boulet *et al.*

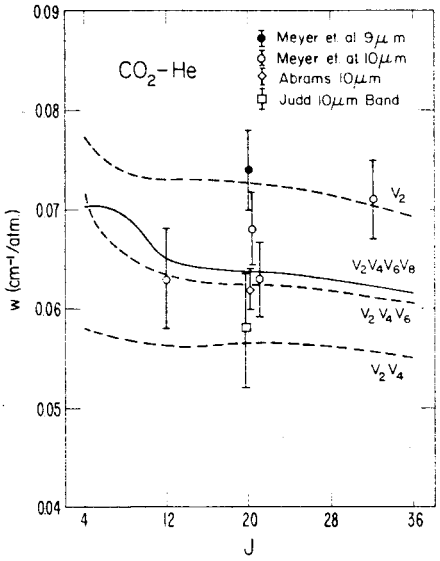

FIG. 6. Linewidths (HWHM) for $j \rightarrow j-1$ transitions in CO_2–He showing the contributions of higher order anisotropy terms in the potential. Terms higher than V_9 have a negligible effect on the linewidth (see discussion in Secs. VI. A and VI. D). Theoretical calculations (solid curve) compare favorably with the measurements of Meyer *et al.*,[30] Abrams,[32] and with experimental data analyzed by Judd.[31]

band. Since Meyer *et al.* point out (on p. 2002) that their 9 μm data seem a bit high, this agreement could be interpreted as closer than that for CO_2–Ar, thereby supporting our assertion that the disparity in the CO_2–Ar case is due to vibrational broadening. As in the CO_2–Ar case, the addition of the V_8 anisotropy raised the calculations by about 2% and the addition of the K_4 term had less than 1% effect.

VII. CONCLUSIONS

We have formulated a new type of exponential approximation for the S-matrix which is designed to be valid for large j values. Our main approximation, introduced in Eqs. (4.1) and (4.2), was the assumption that the change in j in a single V matrix element is small compared with j itself. In the Appendix, it is shown that the error introduced by this approximation is at most the order of $(\Delta j/j)^2$. In our calculations, we have found that the error is usually considerably less than this. For example, in the case of CO–He, the interaction contained terms up to $P_2(\cos\theta)$, so that our error could be as large as $(2/j)^2$. However, for the 1–0 and 2–1 transitions our results lie within 10% of the close coupling results.

Another approximation whose validity is difficult to assess is the use of classical trajectories determined only by the isotropic part, V_0, of the potential. If we were looking directly at the angular distribution of the scattered particles, as in a beam experiment, this approximation would not be adequate. However, for the processes in a gas where one is looking at spherically averaged phenomena, it should be much better. The agreement of our results with close-coupling calculations would tend to support such a conclusion, but this certainly does not constitute a proof. The validity of this approximation should be investigated further.

The main virtue of our approach is that it enables one to use curved classical trajectories which are far more realistic than the straight path trajectories of the Anderson type theories. It also treats the classical path S-matrix to all orders, thereby avoiding the problems attendant with impact parameter cutoffs, etc., which tend to obscure the physical analysis in perturbative approaches such as the Anderson theory.

Apart from close-coupling methods, which are expensive and, for practical purpose, limited to very low quantum numbers, the only other theories which use realistic trajectories and treat the S-matrix to all orders are those classical and semiclassical theories in which the radiating molecule is treated as a classical radiator, usually by means of action angle variables.[23–25] Since one expects this approach to be valid in the limit of high quantum numbers, we were quite surprised to find that our results for CO–He and HCl–He differ by as much as 100% from these classical and semiclassical calculations. We obtained good agreement with semiclassical theories for HCl–Ar but in that case the linewidths are strongly affected by elastic broadening. The use of continuous rather than discrete variables in the classical theories makes it rather difficult to obtain expressions for inelastic transition probabilities and, as discussed in Sec. IV, we suspect that this might be the source of the disagreement for CO–He and HCl–He. In defense of the classical theories, it should be noted that they use classical trajectories which are determined by the full interaction potential and are thus more accurate than ours. We had therefore suspected that our results were in error rather than those of the classical theories; however, the fact that the classical calculations at high j lie above the close-coupling calculations at low j clearly indicates that it is in fact the classical calculations which are in error (linewidths decrease as a function of j owing to a decrease in the inelastic collision cross section).

In the theory of Murphy and Boggs,[5] it is suggested that the linewidths may be regarded as a sum of inelastic cross sections. That is, the elastic term in our equation (5.4) would be ignored. This would be a very useful approximation, if correct, because one could obtain a set of inelastic rates simply by measuring a set of linewidths. This procedure is sometimes used in laser modeling where linewidth measurements are often much easier than direct measurements of inelastic processes.[33] We tested this idea by calculating the elastic and inelastic linewidth contributions separately. For pure rotation lines, we found very little elastic broadening except in the case of HCl–Ar, where the elastic contribution began to approach 50% for the large j values. For all other pure rotation lines, the Murphy–Boggs approximation would have been quite accurate. For vibration–rotation lines, one has to be very careful in applying their approximation because there can be a large elastic contribution from vibrational broadening as there seems to be in the case of CO_2–Ar, for example.

We calculated several linewidths for CO_2–Ar and

CO_2–He using the *ab initio* potentials of Parker *et al.*[19] *Ab initio* potential surfaces such as these typically contain strong contributions from rather high order anisotropies such as $P_4(\cos\theta)$ and $P_6(\cos\theta)$, whereas most semiemperical potentials contain only $P_1(\cos\theta)$ and $P_2(\cos\theta)$ terms. In these calculations we found that the higher order anisotropies influenced the linewidth only through their $\Delta j = 0$ and $\Delta j = 2$ matrix elements. Thus, as far as linewidths are concerned, one could have approximated the effect of the higher order anisotropies by simply changing the $P_2(\cos\theta)$ coefficients. This probably explains why the simple semiempirical potentials are able to give such good agreement with experimental results even though they strongly disagree with *ab initio* calculations.

ACKNOWLEDGMENTS

The authors would like to thank Russel Pack of the Los Alamos Scientific Laboratory for sending us the CO_2–He, Ar potential calculations of Parker *et al.* (1976) in advance of publication. We also wish to thank O'Dean Judd of LASL and D. Truhlar of the University of Minnesota for several useful comments and suggestions. One of the authors (M.G.) wishes to express his gratitude to the Gaseous Electronics Section of the National Bureau of Standards for the hospitality shown him during his stay.

APPENDIX A

In order to discuss the approximations to $\omega_{jj'}$ and $\langle jm|Y_0^l|j'm\rangle$ introduced in Sec. IV, we will consider the second order term in the correct classical path S-matrix [given by Eqs. (2.5) and (3.3)] where these approximations have not been made. The peaking approximation is already built into Eq. (3.3), but that approximation has been shown to be very good by Roberts[11] in cases similar to those encountered here. In line broadening, we are interested only in diagonal S-matrix elements, thus the second order term is

$$S_2 = -\tfrac{1}{2}\mathcal{O}\sum_{j'}\langle jm|\eta'|j'm\rangle\langle j'm|\eta'|jm\rangle$$

$$= -\sum_{ll'j'}\frac{4\pi}{\sqrt{(2l+1)(2l'+1)}}\langle jm|Y_0^l|j'm\rangle\langle j'm|Y_0^{l'}|jm\rangle$$

$$\times\int_{-\infty}^{\infty}e^{i\omega_{jj'}t}V_l(r(t))\,dt\int_{-\infty}^{t}e^{i\omega_{j'j}s}V_{l'}(r(s))\,ds \qquad \text{(A1)}$$

To second order, we can ignore the effect of time ordering because the correction term is imaginary and thus contributes to the line width only when squared (i.e., in fourth order). Furthermore, since our approximations are exact for $j'=j$ (see Sec. IV), we will only consider those terms for which $j'\neq j$.

We first determine the effect of our approximation on $\omega_{jj'}$. If $V(r(t))$ vanishes in a time τ much less than $1/\omega_{jj'}$, any errors due to our approximate $\omega_{jj'}$ may be ignored. The worst possible case (i.e., the most sensitive to $\omega_{jj'}$) is thus when $\omega_{jj'}\tau \gg 1$. To estimate that case let $V(r(t)) = \bar{V}$ for $-\tau \le t \le \tau$ and zero for $|t| > \tau$. We then obtain for the unordered second order integral

$$\frac{1}{2}\int_{-\infty}^{\infty}e^{i\omega_{jj'}t}V_l(r(t))\,dt\int_{-\infty}^{\infty}e^{i\omega_{j'j}s}V_{l'}(r(s))\,ds \simeq 2\left|\int_0^{\tau}\cos(\omega_{jj'}t)\,\bar{V}\,dt\right|^2 \simeq \left(\frac{\bar{V}}{\omega_{jj'}}\right)^2 = \left(\frac{\bar{V}}{2\pi cB}\right)^2\frac{1}{(2j+1-\Delta j)^2\,\Delta j^2}$$

$$= \left(\frac{\bar{V}}{2\pi cB}\right)^2\frac{1}{(2j+1)^2\Delta j^2}\left[1+\left(\frac{\Delta j}{j+\frac{1}{2}}\right)+\frac{3}{4}\left(\frac{\Delta j}{j+\frac{1}{2}}\right)^2+\cdots\right] \qquad \text{(A2)}$$

In the last two lines of Eq. (A2), the exact $\omega_{jj'}$ has been used and the result has been expanded to order $(\Delta j/j)^2$.

The j' sum in Eq. (A1) runs from $j-l$ to $j+l$; thus, Δj will run from $-l$ to $+l$. Consequently, when Eq. (A2) is substituted into Eq. (A1), the odd terms in Δj will vanish. This means that, to order $(\Delta j/j)^2$, we may replace the bracket in Eq. (A2) by unity. This is equivalent to approximating $\omega_{jj'}$ by $2\pi cB(2j+1)\,\Delta j$ [compare the first and third lines of Eq. (A2)]; thus, our $\omega_{jj'}$ approximation is correct to order $(\Delta j/j)^2$. Using this approximation, Eq. (A1) becomes

$$S_2 = -\sum_{ll'j'}\frac{4\pi\bar{V}^2}{\omega^2\,\Delta j^2\sqrt{(2l+1)(2l'+1)}}$$

$$\times\langle jm|Y_0^l|j'm\rangle\langle j'm|Y_0^{l'}|jm\rangle\ , \qquad \text{(A3)}$$

where $\omega = 2\pi cB(2j+1)$ as in Eq. (4.2). The classical expression for the $3j$ symbol used in Eq. (4.1) (see Edmonds[12] or Brussard and Tolhoek[34]) is correct to within terms of order $(\Delta j/j)$; thus, using Eqs. (4.1) and (A3), we have

$$S = -\left(\frac{\bar{V}}{\omega}\right)^2\sum_{ll'j'}\frac{1}{(\Delta j)^2}\frac{(l-\Delta j)!}{(l+\Delta j)!}\frac{(l'-\Delta j)!}{(l'+\Delta j)!}$$

$$\times P_l^{\Delta j}(0)\,P_{l'}^{\Delta j}(0)\,P_l^{\Delta j}\left(\frac{m}{j+\frac{1}{2}}\right)P_{l'}^{\Delta j}\left(\frac{m}{j+\frac{1}{2}}\right)\left[1+A\left(\frac{\Delta j}{j}\right)^2+\cdots\right], \qquad \text{(A4)}$$

where A is a term of order unity or smaller depending on l, l', j, and m and again we have dropped terms proportional to $(\Delta j/j)$ since they cancel out in the sum over j'.

We next consider the second order term in an expansion of our approximate S-matrix, Eq. (4.16) [again assuming $V(r(t)) = \bar{V}$ for $-\tau \le t \le \tau$ and zero for $|t| > \tau$], which is

$$S_2^{\text{approx}} = -2\sum_{\delta>0}K_\delta^2(\omega)$$

$$= \frac{-\bar{V}^2}{\omega^2}\sum_{\delta\neq 0}\sum_{ll'}\frac{1}{\delta^2}\frac{(l-\delta)!}{(l+\delta)!}\frac{(l'-\delta)!}{(l'+\delta)!}$$

$$\times P_l^{\delta}(0)\,P_{l'}^{\delta}(0)\,P_l^{\delta}\left(\frac{m}{j+\frac{1}{2}}\right)P_l^{\delta}\left(\frac{m}{j+\frac{1}{2}}\right)\ , \qquad \text{(A5)}$$

where we have used the fact that the term being summed is invariant under $\delta \to -\delta$ to replace $2\sum_{\delta>0}$ by $\sum_{\delta\neq 0}$, a sum over both positive and negative δ (the limits on this summation are discussed below). We have also omitted the $\delta = 0$ terms since they are identical to the $j = j'$ terms excluded above, and we again used Eq. (A2) to approximate the interaction integrals to order $(\delta/j)^2$.

Since our approximate result, Eq. (A5), is identical to the result obtained from an expansion of an exact S-matrix, Eq. (A4), our approximation would seem to be accurate to within terms of order $(\Delta j/j)^2$. There is, however, one slight complication which must be considered before one can draw this conclusion. The "exact" result, Eq. (A4), contains a sum over intermediate states j' which are restricted by the correct $3j$ symbols, whereas in our exponential approximation, the sum over δ simply runs from $-l$ to $+l$ (or from $-l'$ to $+l'$ if $l' < l$). For example, consider fixed values of m, l, and l' such that $l < l'$. The sum over j' normally ranges from $j - l$ to $j + l$; however, we must also have $j' \geq m$ [see Eq. (A3)], and for large values of m it may happen that $m > j - l$. In that case, j' ranges from m to $j + l$ and δ in Eq. (A5) should run from $-l$ to $j - m$. Unfortunately, there is no such restriction on δ in our approximate S-matrix (this is a general problem with all exponential approximations to S matrices); thus, we are adding in some terms which should not be counted. Fortunately, the terms which are counted incorrectly add only an amount of order $(\Delta j/j)^4$ compared with unity. To show this we note first that the problem occurs only when m is large (i.e., within Δj of $m = j$); thus, in the sum over m [Eq. (5.1)] we are making an error in at most Δj of the $(2j+1)$ terms. If all terms in the sum over m were weighted equally, this error would be at most $(\Delta j/j)$ compared with unity. However, these terms are not weighted equally. For dipole transitions they are weighted by [cf. Eq. (5.1), noting that $j' = j \pm 1$ for dipole transitions] the factor

$$\begin{pmatrix} j & j\pm 1 & 1 \\ m & m' & q \end{pmatrix}^2 \tag{A6}$$

which vanishes for large m. When m is within $|\Delta j|$ of j, Eq. (A6) is $(\Delta j/j)$ smaller than its value at $m = 0$; our error is thus reduced to the order of $(\Delta j/j)^2$ compared with unity. Furthermore, the Legendre polynomials in Eq. (A4) vanish as $1 - m^2/(j+\frac{1}{2})^2$ or faster as $m \to j$. Thus, the terms which are incorrectly included in the summation produce an error the order of $(\Delta j/j)^4$.

We may thus conclude that the error introduced by using the $3j$ symbol approximation of Eq. (4.1), and the approximate frequency $\omega_{jj'} \simeq \omega \Delta j$ of Eq. (4.2) is *at most* the order of $(\Delta j/j)^2$ in the second order term. Since higher order terms are if anything smaller, their error should be relatively less important.

†Supported by the exchange program between the Centre National de la Recherche Scientifique and the National Science Foundation.

*This research was supported in part by ARPA Contract 981 Amendent #9, ERDA Contract E(49-1)-3800, and by National Science Foundation Grant #MPS 72-05169.

[1]P. W. Anderson, Phys. Rev. **86**, 809 (1952).
[2]M. Baranger, Phys. Rev. A **111**, 494 (1958); Phys. Rev. B **112**, 855 (1958).
[3]H. Rabitz, Ann. Rev. Phys. Chem. **25**, 155 (1974).
[4]W. B. Neilsen, and R. G. Gordon, J. Chem. Phys. **58**, 4149 (1973).
[5]J. S. Murphy, and J. E. Boggs, J. Chem. Phys. **47**, 691 (1967).
[6]J. P. Bouanich, and C. Haeusler, J. Quant. Spectrosc. Rad. Transfer **12**, 695 (1972).
[7]R. J. Cross, J. Chem. Phys. **48**, 4838 (1968).
[8]E. W. Smith, J. Cooper, W. R. Chappell, and T. A. Dillon, J. Quant. Spectrosc. Rad. Transfer **11**, 1567 (1971).
[9]R. Pack, J. Chem. Phys. **61**, 2091 (1974).
[10]M. Giraud, D. Robert, and L. Galatry, J. Chem. Phys. **53**, 352 (1970); **59**, 2204 (1973).
[11]R. E. Roberts, J. Chem. Phys. **53**, 1941 (1970).
[12]A. R. Edmonds, *Angular Momentum in Quantum Mechanics* (Princeton U.P., Princeton, NJ, 1960).
[13]It should be noted that the broadening due to "m-changing collisions" (for example, effect #3 discussed by Gordon, Ref. 23) is also included in the present theory even though the S-matrix given in Eq. (4.13) is diagonal in m. This is due to the fact that our coordinate frame is not a space fixed frame such as those usually employed in collision theory. As discussed in Sec. III, for each collision (i.e., for each value of impact parameter and velocity) we rotate to a coordinate frame in which m is conserved for that specific collision. Our coordinate frame is usually referred to as a "collision frame" in the line broadening literature. Our S-matrix in a space fixed frame would be given by $S_{\text{fixed}} = D(-\phi, \theta_0, 0)\, S_{\text{colln}} D^{-1}(-\phi, \theta_0, 0)$, where D is the rotation operator. Since the angle of closest approach, θ_0, is a function of impact parameter velocity, S_{fixed} is a rather complicated *nondiagonal* function of m. Of course the half-width, Eq. (1.1), may be evaluated using either S_{fixed} or S_{colln} since Eq. (1.1) is rotationally invariant. To verify this one may substitute the expression $D^{-1} S_{\text{fixed}} D$ for each S in Eq. (1.1); then, using Eqs. (4.3.2) and (4.2.7) from Edmonds (Ref. 12), one obtains an expression identical to Eq. (1.1) with S_{fixed} in place of S.
[14]I. C. Percival, and D. Richards, J. Phys. B **3**, 1035 (1970).
[15]M. Abramowitz, and I. A. Stegun, Natl. Bur. Stand. Appl. Math. Ser. **55** (1969).
[16]R. G. Gordon, and Y. S. Kim, J. Chem. Phys. **56**, 3122 (1972).
[17]S. Green, J. Chem. Phys. **60**, 2654 (1974).
[18]S. Green and P. Thaddeus, (to be published).
[19]G. A. Parker, R. L. Snow, and R. T. Pack, J. Chem. Phys. **64**, 1668 (1976).
[20]J. Pourcin, thesis, Université de Provence, Marseille, France, 1974.
[21]H. E. Scott, Ph. D. thesis, Ohio State University, 1973.
[22]H. A. Gebbie, and N. W. B. Stone, Proc. Phys. Soc. **82**, 309 (1963).
[23]R. G. Gordon, J. Chem. Phys. **44**, 3083 (1966).
[24]R. G. Gordon and R. P. McGinnis, J. Chem. Phys. **55**, 4898 (1971).
[25]D. E. Fitz and R. A. Marcus, J. Chem. Phys. **62**, 3788 (1975).
[26]S. Green and L. Monchick, J. Chem. Phys. **63**, 4198 (1975).
[27]R. G. Gordon, J. Chem. Phys. **51**, 14 (1969).
[28]C. Roulet, P. Isnard, and E. Arie, J. Quant. Spectrosc. Rad. Transfer **14**, 637 (1974).
[29]R. H. Tipping, and R. J. Herman, J. Quant. Spectrosc. Rad. Transfer **10**, 881 (1970).
[30]T. W. Meyer, C. K. Rhodes, and H. A. Haus, Phys. Rev. **12**, 1993 (1975).
[31]O. P. Judd, Hughes Research Laboratory Report #452, 1971.
[32]R. L. Abrams, Appl. Phys. Lett. **25**, 609 (1974).
[33]O. P. Judd (private communication, 1975).
[34]P. J. Brussard, and H. A. Tolhoek, Physica (Utrecht) **23**, 955 (1957).